



Article

# A Binary Archimedes Optimization Algorithm and Weighted Sum Method for UFLS in Islanded Distribution Systems Considering the Stability Index and Load Priority

Hazwani Mohd Rosli <sup>1,2,\*</sup>, Hazlie Mokhlis <sup>1,\*</sup> , Nurulafiqah Nadzirah Mansor <sup>1</sup> , Norazliani Md Sapari <sup>3</sup>, Syahirah Abd Halim <sup>4</sup>, Li Wang <sup>5</sup> and Mohamad Fani Sulaima <sup>6</sup> 

<sup>1</sup> Department of Electrical Engineering, Faculty of Engineering, Universiti Malaya (UM), Kuala Lumpur 50603, Malaysia; afiqah.mansor@um.edu.my

<sup>2</sup> School of Engineering, Asia Pacific University of Technology and Innovation (APU), Kuala Lumpur 57000, Malaysia

<sup>3</sup> School of Electrical Engineering, Faculty of Engineering, Universiti Teknologi Malaysia (UTM), Johor Bahru 81310, Malaysia; norazliani.ms@utm.my

<sup>4</sup> Department of Electrical, Electronic and Systems Engineering, Faculty of Engineering and Built Environment, Universiti Kebangsaan Malaysia (UKM), Bangi 43600, Malaysia; syahirah\_h@ukm.edu.my

<sup>5</sup> Department of Electrical Engineering, College of Electrical Engineering & Computer Science, National Cheng Kung University, Tainan City 70101, Taiwan; liwang@mail.ncku.edu.tw

<sup>6</sup> Faculty of Electrical Engineering, Universiti Teknikal Malaysia Melaka, Melaka 76100, Malaysia; fani@utem.edu.my

\* Correspondence: hazwani@apu.edu.my (H.M.R.); hazli@um.edu.my (H.M.)

**Abstract:** This study proposes an under-frequency load-shedding (UFLS) scheme based on a binary Archimedes Optimization Algorithm (BAOA) and the Weighted Sum Method (WSM) to maintain the stability of an islanded distribution system. These methods consider stability indices and load priorities to ensure effective load shedding during frequency deviations. The BAOA determines the optimal load shedding based on the stability index and power mismatch that minimizes the impact on critical loads while maintaining system stability in an islanded distribution system. The WSM determines the rank of the load to be shed based on four criteria: the load priority, the load category, the stability index, and the load size. Each load is assigned a weight based on its priority. These weight variables determine the order in which loads are shed during frequency deviations. The effectiveness of the proposed UFLS was tested on an 11 kV Malaysian distribution network with two mini hydro distributed generation systems. A comparative study was conducted based on five result outputs, including the number of loads shed, the size of the loads shed, the frequency undershoot, the frequency overshoot, and the time taken to achieve a stable frequency in three cases: base load, peak load, and peak load with photovoltaics (PV). The proposed UFLS showed the best results for 11 of 15 outputs (73.3%) for islanding events and 9 of 15 outputs (60%) for overloading events. The voltage profile and stability index, also, were improved after the proposed UFLS was applied.

**Keywords:** under-frequency load shedding; islanded distribution system; frequency response; stability index; Archimedes Optimization Algorithm; Weighted Sum Method



**Citation:** Mohd Rosli, H.; Mokhlis, H.; Mansor, N.N.; Md Sapari, N.; Halim, S.A.; Wang, L.; Sulaima, M.F. A Binary Archimedes Optimization Algorithm and Weighted Sum Method for UFLS in Islanded Distribution Systems Considering the Stability Index and Load Priority. *Energies* **2023**, *16*, 5144. <https://doi.org/10.3390/en16135144>

Academic Editor: Javier Contreras

Received: 27 May 2023

Revised: 19 June 2023

Accepted: 29 June 2023

Published: 3 July 2023



**Copyright:** © 2023 by the authors. Licensee MDPI, Basel, Switzerland. This article is an open access article distributed under the terms and conditions of the Creative Commons Attribution (CC BY) license (<https://creativecommons.org/licenses/by/4.0/>).

## 1. Introduction

According to [1], Malaysia consumes 4721 kWh per capita, with natural gas and coal dominating power generation at 39.8% and 36.7%, respectively. This results in high average carbon emissions. Thus, the government has established a target of a 31% renewable energy contribution to the national installed capacity mix by 2025 [2]. In 2019, the installed capacities for renewable energy in Malaysia were 2.9%, 0.4%, and 1.2%, respectively. Considering clean, low-impact sources of energy, reduced emissions, and improved grid resilience, many studies have been conducted to facilitate the integration of distributed generation

(DG) into power-system networks. Nevertheless, a major concern in DG operations is the possibility of an islanded distribution system. Islanding in a distribution system is an event in which part of the utility system is electrically isolated from the main grid owing to a fault upstream or any other disturbance but remains energized by the DG connected to it. The occurrence of unintentional islanding causes numerous problems for DG and maintenance personnel. Owing to power imbalance, DG is likely to be out of synchronism, resulting in abnormal voltage and frequency with respect to the utility load, which could be detrimental to consumers [3]. Thus, several studies have been conducted on under-frequency load shedding (UFLS) to address the issue of power imbalance during islanding events.

UFLS disconnects certain loads when the system frequency decreases below a pre-determined threshold. This allows the system frequency to be restored to an acceptable level without risking system stability. UFLS is divided into three categories: conventional, adaptive, and computational-intelligence-based strategies [4,5]. Adaptive load shedding measures the frequency decline rate or the Rate of Change of Frequency (ROCOF) to estimate the disturbance magnitude based on power imbalance in the system [6–9]. The integration of ROCOF and the ranked stability index for a UFLS scheme in [10] offers a promising approach to enhance system stability and ensure reliable operations. However, the combination for load shedding does not include load priority in the ranking of loads shed. The new UFLS scheme proposed in [11] incorporates the locally estimated ROCOF of the Center of Inertia (COI) in load-shedding strategies. Nevertheless, this study addresses the need for the integration of intelligent algorithms to enhance load-shedding performance.

Intelligent load-shedding techniques have been developed to improve the accuracy and effectiveness of the frequency control method required to maintain system stability. In [12], hybrid meta-heuristic techniques were applied for optimal load-shedding planning and operations in islanded distribution networks. This study explored the advantages of combining multiple meta-heuristic algorithms to overcome their individual limitations and enhance overall performance. However, it did not sufficiently consider the transient behavior of the system during load-shedding events. The UFLS scheme in [13] employs polynomial regression and mixed-integer linear programming (MILP) to forecast power imbalances in the system. Nevertheless, owing to the enormous search space required, this method cannot provide a feasible solution for larger test systems. References [14,15] proposed a load shedding scheme based on voltage stability indices for islanded distribution systems. The authors utilized the voltage collapse point as indices to determine the criticality of loads during voltage fluctuations. However, these studies did not provide frequency response or a detailed discussion of the prioritization criteria for load shedding. Different types of loads may have varying criticality levels, and the scheme should account for this in determining which loads to shed first.

Fuzzy logic was applied in [16] to overcome the limitations of traditional UFLS techniques by adaptability to change in system conditions. The integration of the Grasshopper Optimization Algorithm GOA in smart load-management systems enables intelligent decision making for load shedding [17]. The algorithm can adaptively determine the optimal amount of load shedding based on real-time data, load characteristics, and grid conditions, thereby improving system reliability and minimizing energy waste.

In [18], the integration of a modified Discrete Evolutionary Programming (DEP) algorithm with the Analytical Hierarchy Process (AHP) technique, incorporating stability indices, offers a promising approach to enhance the effectiveness of load-shedding schemes. By considering the criticality of loads and system stability simultaneously, these schemes provide a more comprehensive solution for load-shedding optimization. However, these studies did not consider load priority, which is important to prevent loss of supply for critical loads, as well as stability indices, where load shedding can be initiated at an appropriate level to prevent further deterioration of the system's stability.

Although UFLS systems have been shown to be effective in maintaining system stability, they can also disrupt consumers who are directly affected by the shed load. Considering the implications of both system reliability and consumer priority, this study

proposes a UFLS based on the binary Archimedes Optimization Algorithm (BAOA) and Weighted Sum Method (WSM) to identify the best solution for the load to be shed. The main contributions of this study are as follows:

1. The proposed binary technique in the AOA selects the best load shed based on the minimum stability index and power mismatch.
2. The proposed UFLS scheme employs a WSM to rank the load shed based on load priority, load category, stability index, and load size.
3. The proposed UFLS scheme improves the frequency response, increases the voltage stability, and reduces the load shed by considering the power reserve of the mini hydro DG.

The remainder of this paper is organized as follows. Section 2 presents the proposed BAOA for selecting the optimal load shed for the load priority. Section 3 describes the modeling of the proposed UFLS in a system based on a BAOA and WSM. Section 4 describes the existing distribution system used as the test system and case study. Section 5 presents and discusses the results. Finally, Section 6 concludes the paper.

## 2. Load Priority Using Binary AOA

The Archimedes Optimization Algorithm (AOA) proposed in [19] is an iterative optimization algorithm used to solve nonlinear problems. AOA is particularly beneficial because of its ability to solve problems with many variables or complex constraints which cannot be easily solved using traditional methods. However, the load-shedding scheme is a discrete problem in which the objective function and constraints are integer-valued. Therefore, a BAOA is proposed in this study to determine the best and minimum combination of loads to be shed and consequently predict the effects of load shedding on the other parts of the system.

Each load in the distribution system is represented by a binary variable that indicates whether the load should be shed (1) or not (0) during frequency deviations. Stability index as a constraint ensures that the system stability index remains within an acceptable range during and after frequency deviations. Considering load priority via the stability index also assists in shedding loads in a way that minimizes the impact on critical loads. Critical loads should be shed first to maintain system reliability. Therefore, the fitness function proposed in this study evaluates the quality of a load-shedding scheme based on the stability index and load priorities. It quantifies the deviation from the desired stability index and penalizes the shedding of critical loads.

### 2.1. Binary AOA

The following are the proposed BAOA steps for the load-shedding scheme. The nonbinary Formulae (1) to (10) are as in [19].

#### Step 1: Initialization

The generation of a random set of particles or solutions consists of the number of buses of connected load, as shown in (1).

$$\begin{aligned}x_i &= randi() \\den_i &= rand() \\vol_i &= rand() \\acc_i &= lb_i + rand() \times (ub_i - lb_i)\end{aligned}\tag{1}$$

where  $randi()$  are integer numbers generated as either 0 or 1 for each particle  $i$ ;  $den$  and  $vol$  are the density and volume, respectively; and  $rand()$  generates random numbers in the range of  $[0, 1]$ .  $acc$  is particle acceleration, where  $ub$  and  $lb$  are the upper and lower boundaries of the search space, respectively. The particles, density, volume, and acceleration are generated in the vector dimension of  $d$  and with a population size of  $N$ .

### Step 2: Updating density and volume

The density and volume of each particle  $i$  for iteration  $t$  are updated, as shown in (2) and (3), respectively.

$$den_i^{t+1} = den_i^t + rand \times (den_{best} - den_i^t) \quad (2)$$

$$vol_i^{t+1} = vol_i^t + rand \times (vol_{best} - vol_i^t) \quad (3)$$

where  $den_i$ ,  $vol_i$ , and  $acc_i$  are the density, volume, and acceleration, respectively, of the  $i$ th particle at iteration  $t$  and  $den_{best}$  and  $vol_{best}$  are the density and volume of the best particle, respectively.

### Step 3: Updating acceleration

The acceleration is updated based on two operators, namely, the transfer operator,  $TF$ , and the density operator,  $d$ , as in (4) and (5), respectively, where the transfer operator transforms the search from exploration to exploitation, whereas the density operator assists the global search for the local search.

$$TF = \exp\left(\frac{t-T}{T}\right) \quad (4)$$

$$d = \exp\left(\frac{t-T}{T}\right) - \left(\frac{t}{T}\right) \quad (5)$$

When  $TF \leq 0.5$ , the acceleration is updated based on the exploration phase, whereas when  $TF > 0.5$ , it is updated based on the exploitation phase, as shown in (6) and (7), respectively. The acceleration is normalized, as shown in (8).

$$acc_i^{t+1} = \frac{den_r + vol_r \times acc_r}{den_i^{t+1} \times vol_i^{t+1}}; TF \leq 0.5 \quad (6)$$

$$acc_i^{t+1} = \frac{den_{best} + vol_{best} \times acc_{best}}{den_i^{t+1} \times vol_i^{t+1}}; TF > 0.5 \quad (7)$$

$$acc_{i-norm}^{t+1} = u \times \frac{acc_i^{t+1} - \min(acc)}{\max(acc) - \min(acc)} + l \quad (8)$$

where  $den_r$ ,  $vol_r$ , and  $acc_r$  are the density, volume, and acceleration of the selected random particle, respectively;  $acc_{best}$  is the acceleration of the best particle; and  $u$  and  $l$  are the ranges of normalization, which are set to 0.9 and 0.1, respectively.

### Step 4: Updating position

The new positions of the particles in the population are updated, as shown in (9) and (10).

$$x_i^{t+1} = \begin{cases} x_i^t + C1 \times rand \times acc_{i-norm}^{t+1} \times (x_{rand} - x_i^t) \times d & \text{if } TF \leq 0.5 \\ x_{best}^t + f \times C2 \times rand \times acc_{i-norm}^{t+1} \times (T \times x_{best} - x_i^t) \times d & \text{if } TF > 0.5 \end{cases} \quad (9)$$

$$f = \begin{cases} +1 & \text{if } P \leq 0.5 \\ -1 & \text{if } P > 0.5 \end{cases} P = 2 \times rand - C4 \quad (10)$$

where  $C1$  and  $C2$  are constants with the values 2 and 6, respectively;  $T = C3 \times TF$  and  $f$  is the flag parameter defined in (10); and  $C3$  and  $C4$  are constants with the values 2 and 0.5, respectively. However, to update the positions of the particles in a discrete search space, a

sigmoidal transfer function [20] is implemented in the BAOA, as shown in (11). Therefore, the updated position of the particles in the BAOA is  $x'$ , which is within the limited range of  $[0, 1]$ , as shown in (12).

$$\text{sig}(x_i^{t+1}) = \frac{1}{1 + e^{-(x_i^{t+1})}} \quad (11)$$

$$x_i^{t+1} = \begin{cases} 0 & \text{if } \text{rand} \geq \text{sig}(x_i^{t+1}) \\ 1 & \text{if } \text{rand} < \text{sig}(x_i^{t+1}) \end{cases} \quad (12)$$

## 2.2. Proposed Fitness Function

In this study, the fitness function for the BAOA to solve the UFLS is proposed to select both the minimum stability index (SI) and the optimal size of the load to be shed, as shown in (13) and (14), respectively. The value of the stability index is based on the load selected in (12). A penalty is introduced in the fitness function to ensure that the load selection does not violate the power imbalance, as expressed in (14). The balance between generation and load is important to avoid unnecessary overshooting in the system frequency owing to the excessive load shed in the system. Thus, the optimal size of the load shed is based on the minimum mismatch between the total load selected and the total generation of the DG, which is introduced as a penalty in (15) and (16), respectively. To cater to the power loss from the grid, the total generation by the mini hydro must first consider the power reserve to reduce the number of loads to be shed. Therefore, this study proposes considering the difference in the power generated by the mini hydro before and after islanding,  $\Delta P_{DG}$ , to allow the release of the power reserve.

$$\text{Fitness} = \sum_{n=1}^{nload} SI \times (1 + q * \text{Penalty}) \quad (13)$$

$$SI = 2V_s^2 V_r^2 - V_r^4 - 2V_r^2 (PR + QX) - |Z|^2 (P^2 + Q^2) \quad (14)$$

$$\text{Penalty} = \max(\text{Mismatch} / \Delta P_{DG}, 0) \quad (15)$$

$$\text{Mismatch} = \Delta P_{DG} - \sum_{n=1}^{nload} P_{load} \quad (16)$$

where  $V_s$  and  $V_r$  are the sending and receiving end voltages, respectively;  $P$  and  $Q$  are the active and reactive loads, respectively;  $R$  and  $X$  are the line resistance and reactance, respectively;  $Z$  is the impedance of the line;  $nload$  is the total number of loads selected; and  $q$  is a constant for the penalty.  $\Delta P_{DG}$  is the difference in power before and after the grid disconnection.  $P_{load}$  is the total power consumed by the selected load.  $SI = 1.0$  means stable, while  $SI = 0.0$  means critical stability.

## 3. The Proposed UFLS Using BAOA and WSM

To maintain system stability while minimizing the load shed, this study introduces a UFLS approach that combines optimization and multi-criteria decision-making methods. Specifically, the Load Selection Module (LSM) employs the BAOA to identify the minimum number of loads with the least power imbalance and the lowest stability index. From the nonvital load options, only the best solution selected by BAOA is transferred to the Load Ranking Module (LRM), which utilizes the Weighted Sum Method (WSM) to determine the shedding sequence of loads. The ranked load list is then passed to the Load-Shed Controller Module (LSCM), which activates the corresponding remote circuit breaker (RCB) for load disconnection. It is assumed that the distribution system is equipped with reliable monitoring devices for measurement units and RCBs. The proposed UFLS process is visually depicted in Figure 1. To validate the effectiveness of the proposed scheme in

the distribution system, modeling and simulation were conducted using PSCAD/EMTC and MATLAB.

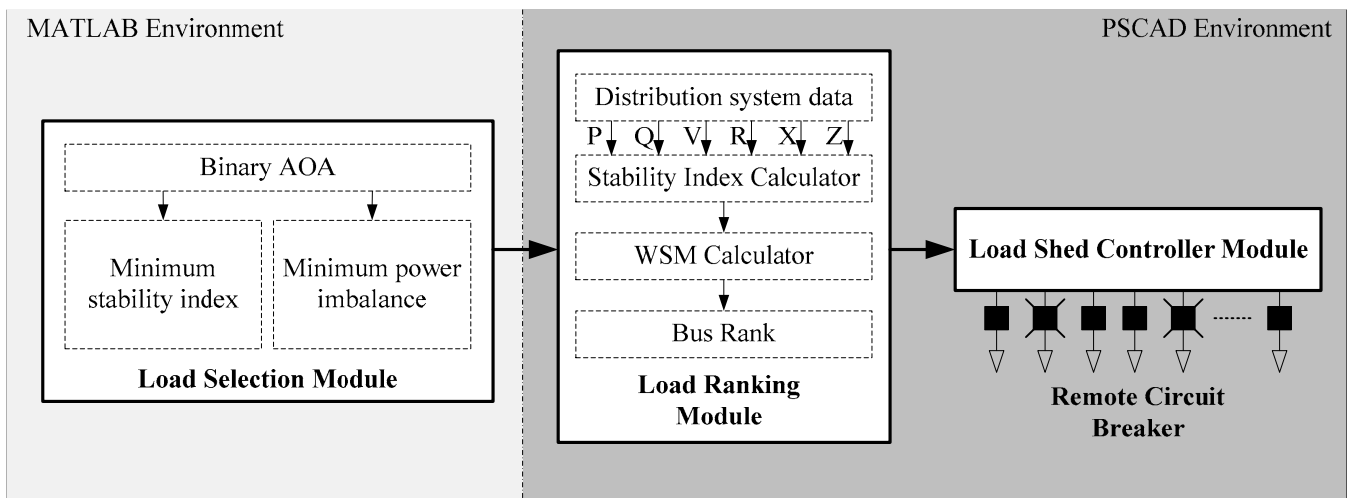


**Figure 1.** Layout of the proposed UFLS using BAOA and WSM.

In LRM, the Stability Index Calculator (SIC) computes the voltage stability index based on the actual distribution system data using (14), as introduced in [21] for radial distribution networks. The voltage stability index is considered in the proposed UFLS to identify the critical buses during the system instability caused by the loss of generation from the grid. Subsequently, the rank of the load to be shed is acquired based on the WSM weightage, considering four criteria: the load selected by the BAOA, the stability index, the load size, and the load category. The load category comprises vital, semi-vital, and nonvital loads.

### 3.1. The Weighted Sum Method (WSM) in the Load Ranking Module (LRM)

A multi-criteria decision-making method is applied to determine the best decision regarding the priority of the loads to be shed. The WSM evaluates the alternatives (loads to be shed) based on four criteria: load priority (load selected by the BAOA), load category, stability index, and load size. The elements of the load-priority criterion are based on power mismatch in (16) obtained from the BAOA. The elements of the buses that are not selected by the BAOA are assigned values equal to those of the elements in the load category. In the load-category criterion, the numerical values of  $x_1$ ,  $x_2$ , and  $x_3$  are assigned to represent the nonvital, semi-vital, and vital loads, respectively, where  $x_1 < x_2 < x_3$ . The elements of the stability index are based on (14) for each bus. The elements of the load-size criterion are based on the load demand for each bus. Table 1 shows a sample array with the element values assigned for each bus to calculate the criteria weights and alternative weights.

**Table 1.** Four criteria considered in LRM based on WSM.

Bus	Load Priority	Load Category	Stability Index	Load Size (MW)	Score
1	$P_{mismatch}^1$	$x_1^1$	$SI^1$	$Load^1$	$W^1$
⋮	$P_{mismatch}^{ith}$	$x_1^{ith}$	$SI^{ith}$	$Load^{ith}$	$W^{ith}$
11	$x_1^{11}$	$x_1^{11}$	$SI^{11}$	$Load^{11}$	$W^{11}$

Table 1. Cont.

Bus	Load Priority	Load Category	Stability Index	Load Size (MW)	Score
12	$x_2^{12}$	$x_2^{12}$	$SI^{12}$	$Load^{12}$	$W^{12}$
$\vdots$	$x_2^{ith}$	$x_2^{ith}$	$SI^{ith}$	$Load^{ith}$	$W^{ith}$
23	$x_3^{23}$	$x_3^{23}$	$SI^{23}$	$Load^{23}$	$W^{23}$
$\vdots$	$x_3^{23}$	$x_3^{23}$	$SI^{ith}$	$Load^{ith}$	$W^{ith}$
$nbus$	$x_3^{nbus}$	$x_3^{nbus}$	$SI^{nbus}$	$Load^{nbus}$	$W^{nbus}$

The following are the steps to determine the criteria and the alternative weighting for the decision regarding the ranking of the loads to be shed:

### 3.1.1. Criteria Weights Using the Entropy Method

In this study, the WSM employs the entropy method to calculate the criteria weightings in lieu of predetermined values before the alternatives are evaluated. Each of the four criteria is assigned a weight based on the entropy method to determine the importance of the criteria as follows:

1. The arrays of the decision matrix (criteria for each load) are normalized to obtain the common scale values for the elements of the different criteria, as shown in (17).

$$r_{ij} = \frac{x_{ij}}{\sum_{i=1}^{nbus} x_{ij}} \quad (17)$$

where  $x$  is the performance value of the decision matrix according to the  $j$ th criteria for load priority, stability index, load size, and load category for the  $i$ th alternative load and  $nbus$  denotes the total number of buses with the connected loads.

2. The entropy of the normalized elements in the decision matrix is computed as in (18).

$$e_j = -h \sum_{i=1}^{nbus} r_{ij} \ln r_{ij} h = \frac{1}{\ln(nbus)} \quad (18)$$

3. The weighting of each criterion is defined based on the entropy method as in (19).

$$cw_j = \frac{1 - e_j}{\sum_{j=1}^m (1 - e_j)} \quad (19)$$

### 3.1.2. Alternative Weights Using the WSM

The values from the entropy method are applied to the WSM to compute an alternative weighting and score for each bus load as follows:

1. Identify the criteria as either beneficial or nonbeneficial to determine whether maximum or minimum values are required. The decision matrix is normalized according to the beneficial and nonbeneficial criteria, as shown in (20) and (21), respectively.

$$b_{ij} = \frac{\min(x_{ij})}{x_{ij}} \quad (20)$$

$$nb_{ij} = \frac{x_{ij}}{\max(x_{ij})} \quad (21)$$

where  $b$  is the element of the decision matrix that is preferred to have higher values and  $nb$  is the element of the decision matrix preferred to have lower values.

- Convert to the weighted normalized decision matrix by multiplying both beneficial and nonbeneficial elements of the decision matrix by each criterion’s weight and summing the elements of all criteria for each alternative. The rank of each load to be shed is obtained from the score for each alternative,  $A_{ij}$ , as shown in (22) and (23).

$$A_{ij} = \sum_{j=1}^m cw_j b_{ij} \tag{22}$$

$$A_{ij} = \sum_{j=1}^m cw_j nb_{ij} \tag{23}$$

The summary of the WSM which comprises the criteria and alternative weightings is presented in Figure 2.

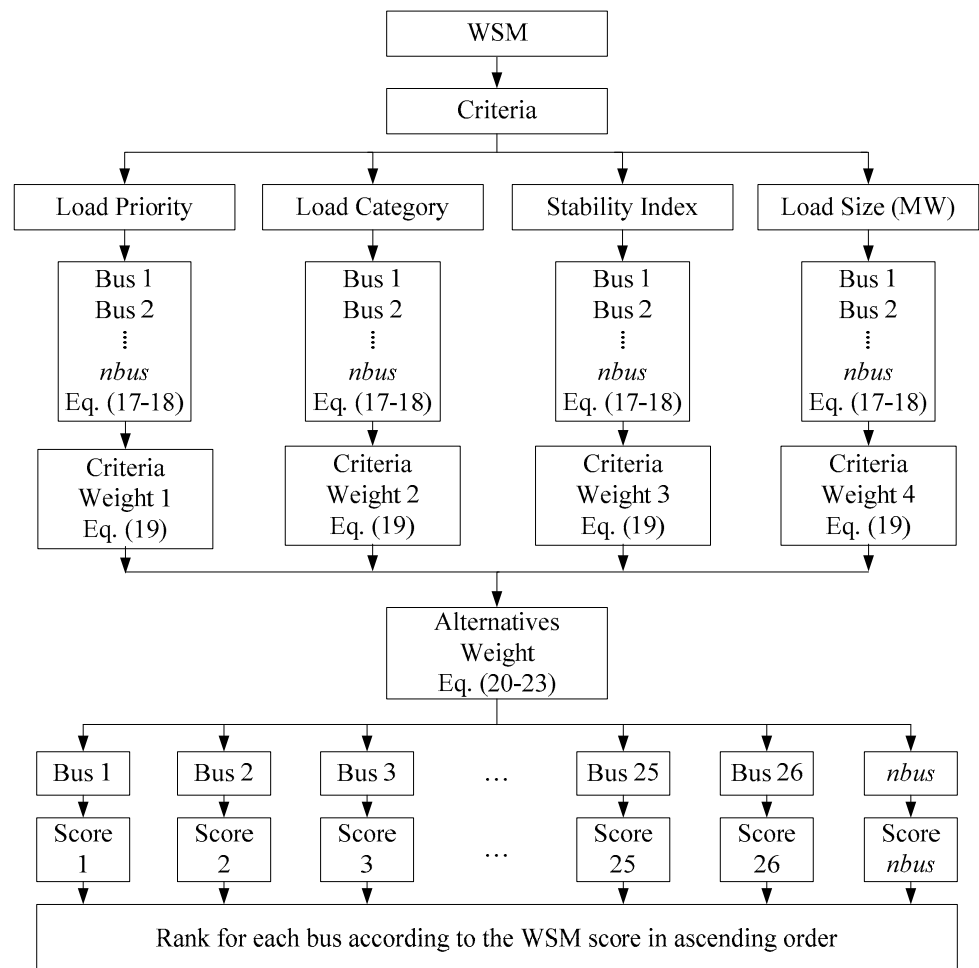


Figure 2. Block diagram of the WSM comprises criteria and alternative weightings.

### 3.2. Load-Shed Controller Module (LSCM)

The load-shed controller module (LSCM) has been developed to oversee islanding occurrences and subsequent instances of overloading. Additionally, the LSCM governs the location and number of breakers to be opened based on the load-shedding priority determined by the Weighted Sum Method (WSM) in the Load Ranking Module (LRM). By monitoring the system frequency and power imbalance, the LSCM assesses the necessary load-shedding location. In the event of an islanding, the LSCM identifies the absence of grid power supply and detects the power imbalance between supply and demand, as indicated in (24). To compensate for power loss, the LSCM also examines the availability of spinning reserve through mini hydro DGs. However, if the spinning reserve is insufficient,



the LSCM transmits a signal to the relevant remote circuit breaker (RCB) to disconnect the load. The LSCM proceeds to shed loads from the list provided by the LRM until the system frequency stabilizes and the power imbalance approaches zero. As per [22], the network’s system frequency should be maintained within 50 Hz ± 1%. Consequently, the LSCM ceases load shedding when the system frequency,  $F$ , exceeds the tolerance frequency,  $f_t$ , of 49.5 Hz.

$$\Delta P = (P_{grid} + P_{DG} + P_{reserve}) - (P_{load} + P_{losses}) \tag{24}$$

In an overloading event, the total power imbalance arising from a sudden load increase in the network system is calculated using the swing equation, taking into account the magnitude of the Rate of Change of Frequency (ROCOF), as described in (25). The load-shedding procedure for sudden overloading is initiated only if the estimated power imbalance surpasses a predefined threshold. The LSCM diligently monitors the network for any irregular conditions, such as overload or excessive power generation.

$$\Delta P = \left( 2 \times \sum_{i=1}^{N_{DG}} H_i / f_n \right) \times df_c / dt \tag{25}$$

where  $H_i$  is the inertia constant of the  $i$ th generator,  $f_n$  is the rated frequency,  $N_{DG}$  is the number of DGs, and  $df_c / dt$  is the rate of change of the center inertia frequency. A flowchart of the LSCM operation is presented in Figure 3.

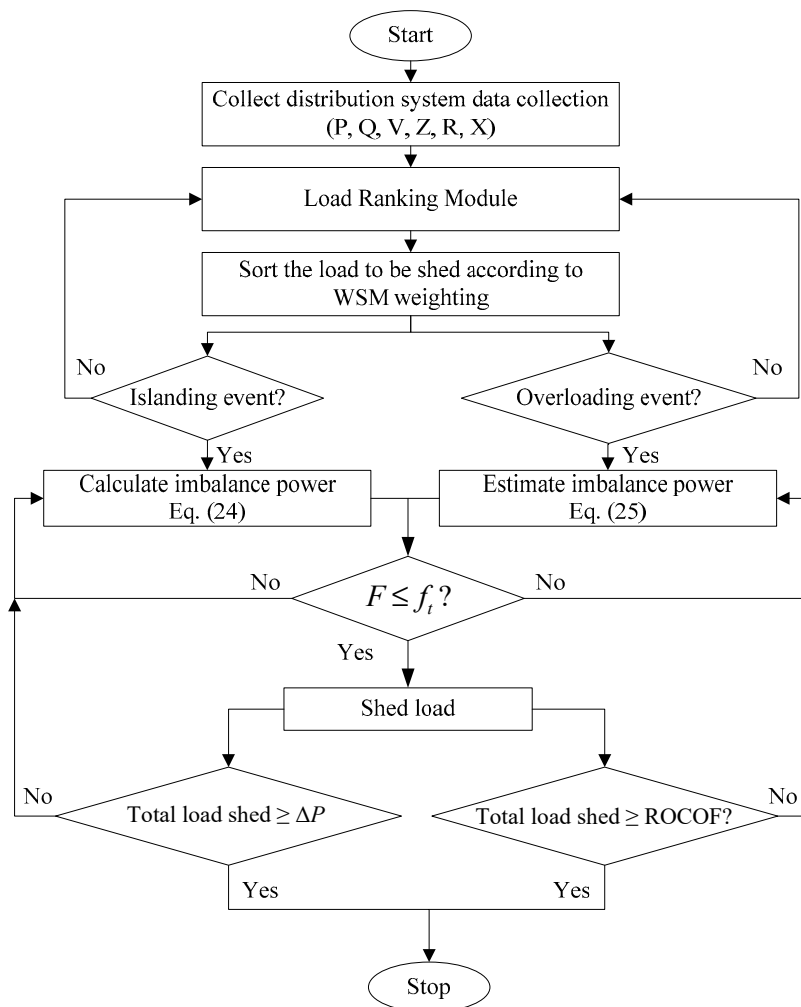


Figure 3. Flowchart of LSCM for both islanding and overloading events.

### 4. Test-System Modeling

The proposed UFLS scheme was tested on an existing 11 kV Malaysian actual distribution network, as shown in Figure 4. The distribution system consisted of 30 buses with two mini hydro synchronous generators and PV generators. The distribution network was connected to the grid via two step-down 132 kV/11 kV transformers and two MVA transformers. Each unit of the mini hydros was rated at 2 MVA with a maximum power dispatch of 1.8 MW and step up via a 2 MVA, 3.3 kV/11 kV transformer.

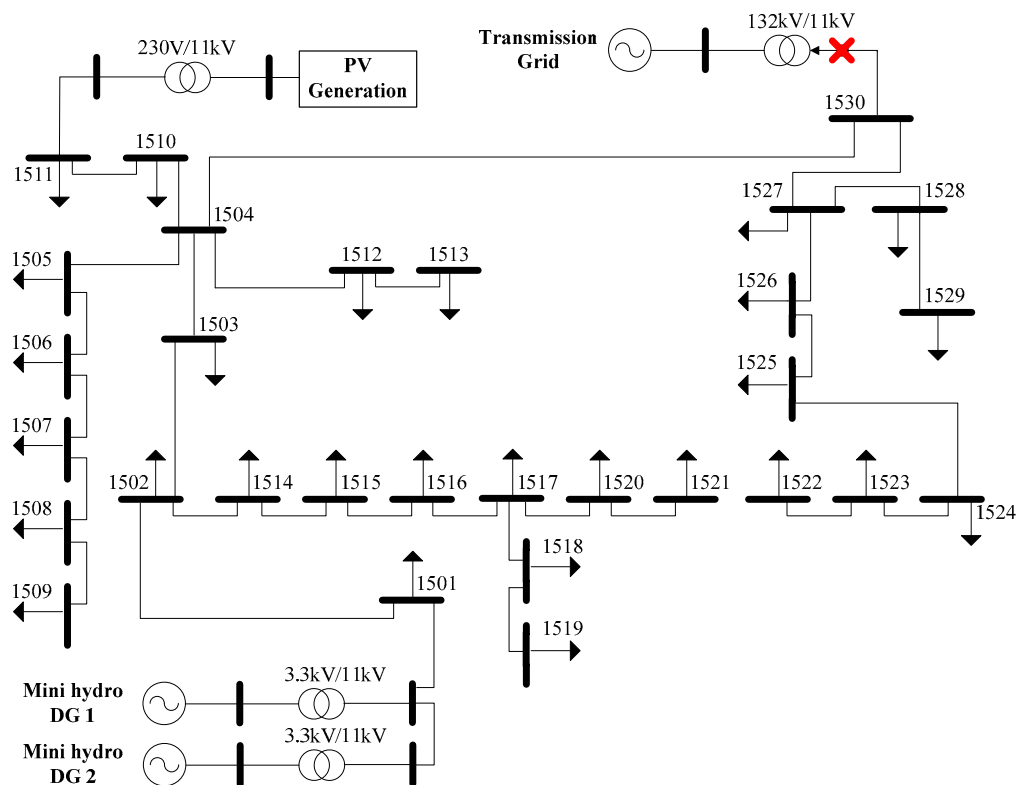


Figure 4. Existing 11 kV Malaysian distribution network.

The maximum power generated by PV is 0.2 MW and step up is via a 230 V/11 kV transformer. The load connected was categorized into 11 nonvital, 11 semi-vital, and 5 vital loads, as shown in Table 2. To evaluate the performance of the proposed UFLS, three case studies were considered, as listed in Table 3. The total demand in the system includes both the loads and losses.

Table 2. Category of loads.

Category	Loads Connected (Buses)
Nonvital	1502, 1503, 1506, 1510, 1511, 1515, 1518, 1519, 1522, 1525, 1526
Semi-vital	1505, 1507, 1508, 1509, 1513, 1514, 1517, 1520, 1523, 1524, 1527
Vital	1501, 1516, 1521, 1528, 1529

Table 3. Total demands for the test system.

Case Study	Generation	Total Demand
Case 1	2 mini hydros	3.11 MW
Case 2	2 mini hydros	3.74 MW
Case 3	2 mini hydros and PV generation	3.74 MW

## 5. Results and Discussion

To verify the performance of the proposed UFLS using the BAOA and WSM, simulations were conducted for two events: islanding and overloading, as described in Table 4. Islanding was simulated by disconnecting the incoming substation at 3.5 s. In the overloading event, a sudden increase in the 0.5 MW load was connected to the system at 40.0 s during islanding to validate the efficacy of the LSCM in monitoring the power imbalance. The following performance tests were conducted for the three case studies in two event modes:

Test 1: Frequency response without UFLS;

Test 2: Frequency response with UFLS using individual stability indices and load sizes;

Test 3: Comparison of the frequency responses and load shedding for Case 1;

Test 4: Comparison of the frequency responses and load shedding for Case 2;

Test 5: Comparison of the frequency responses and load shedding for Case 3;

Test 6: Voltage profile and stability index of the proposed UFLS.

**Table 4.** Events for UFLS.

<b>Islanding Event</b>	Main utility grid is disconnected at 3.5 s after normal operation is stabilized
<b>Overloading Event</b>	Sudden overloading occurs subsequently, after 40 s

The lists of the rankings of the loads to be disconnected according to the computed scores are shown in Appendix A. The proposed scheme prioritizes the nonvital load to be shed, followed by the semi-vital and nonvital loads. The rankings for Cases 2 and 3 were similar, owing to the same load demand of the test system. The efficacy of the load rank using the proposed scheme is assessed based on the frequency response in the next section.

### 5.1. Frequency Response without UFLS

To evaluate the performance of the proposed UFLS in different scenarios, the test system considered the base and peak load demands at 3.11 MW and 3.74 MW, respectively. The impact of islanding on the system's frequency is shown in Figure 5, where the grid is disconnected from the test system and no load-shedding scheme is implemented. The frequency response was significantly reduced owing to the sudden disruption of the power supply from the main grid for both the load demands.

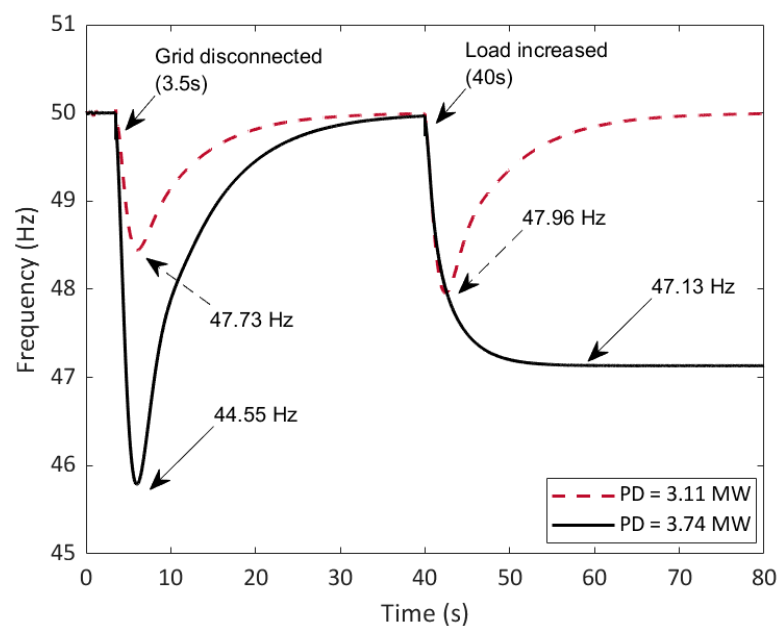


**Figure 5.** Frequency response based on 3.11 MW and 3.74 MW total load demands.

At a 3.11 MW load demand, the frequency dropped to 47.73 Hz but recovered at 30.5 s, while at 3.74 MW the frequency dropped to 44.55 Hz but recovered at 40.0 s. Although the frequency recovered eventually, it took an extended period of time. The instability of the system became more apparent with increasing load in the islanded distribution system at 40 s. At a 3.11 MW load demand, the frequency response dropped to 47.96 Hz but recovered at 65 s, while at 3.74 MW the frequency dropped to 47.13 Hz but did not recover, as the power supply from the DG system had reached its maximum reserve and was no longer capable of meeting the high load demand.

### 5.2. Frequency Response with UFLS Using Individual Stability Index and Load Size

To justify the significance of both the stability index and load size considered in the load-shedding scheme, frequency responses based on stability indices and load sizes were recorded independently, as shown in Figure 6, for the islanding and overloading events, respectively. The load shedding was based on the ascending order of either the stability indices or the load-size values. In the UFLS based on SI, the buses with minimum stability indices were critical; thus, they were shed first. In UFLS based on load size, the buses with minimum load sizes were shed first to reduce the probability of over-shedding. It is shown in Figure 6a that UFLS based on load size had a frequency overshoot of 50.12 Hz and recovered to a stable frequency at 34.57 s, while UFLS based on SI reached approximately a 50.0 Hz frequency at 28.5 s. In contrast, the proposed UFLS, which considers both the stability index and load size, had no frequency overshoot and was able to recover at 16.47 s.

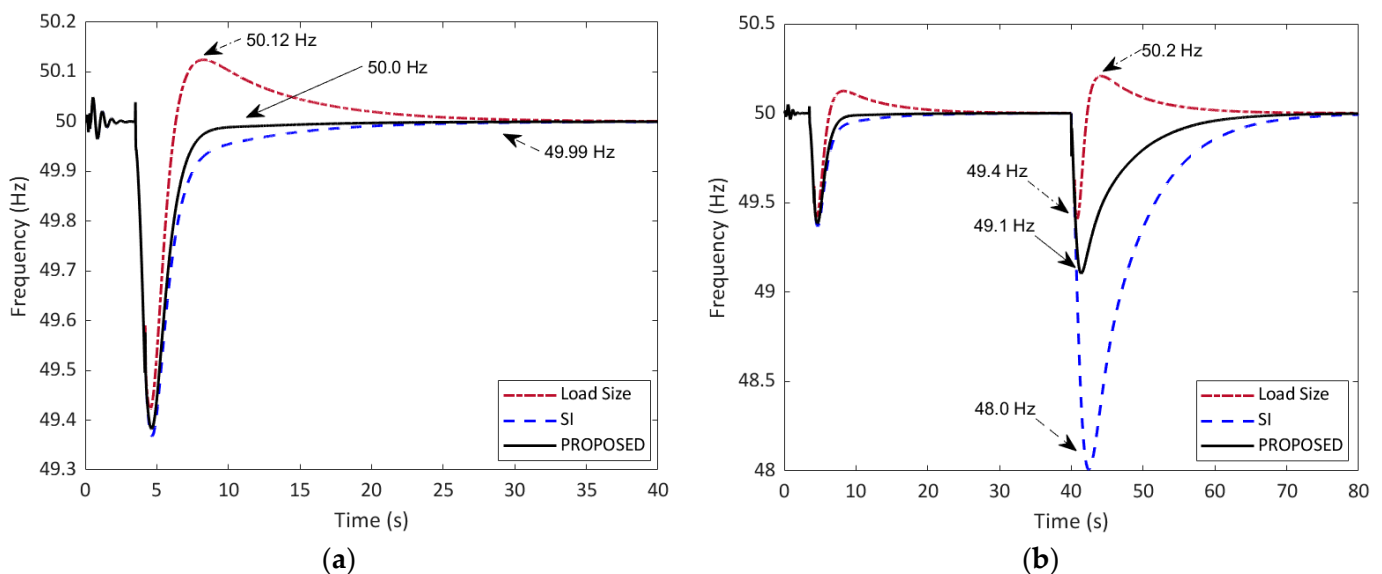


**Figure 6.** Frequency response based on individual load size and stability index in (a) islanding events and (b) overloading events.

In the overloading event, UFLS based on load size had a frequency overshoot of 50.2 Hz and recovered to a stable frequency at 73.9 s, while the UFLS based on SI had no frequency overshoot and recovered at 77.93 s, as shown in Figure 6b. However, the UFLS based on SI had the lowest frequency undershoot of 48.0 Hz as compared to other approaches for islanding events. Despite having a lower frequency undershoot compared to the UFLS based on load size, the proposed UFLS had no frequency overshoot and recovered the fastest at 68.03 s. In summary, it was observed that consideration of the stability index is more significant in an islanding event, whereas consideration of the load size is more significant in an overloading event. Thus, the proposed UFLS considers both the stability index and the load size to determine the rank of the load shed using the BAOA and WSM techniques.

### 5.3. Comparison of the Frequency Responses and Load Shedding for Case 1

A comparison with the adaptive technique [8,23] and UFLS<sub>PSI</sub> [10] approaches was conducted to validate the performance of the proposed UFLS based on BAOA and WSM. The adaptive technique in [8,23] predetermined the list of loads to be shed with no stability index. The UFLS<sub>PSI</sub> [10] approach considers the power stability index (PSI) and only the nonvital load to be shed. However, for comparison purposes, the UFLS<sub>PSI</sub> [10] approach was modified to consider all load categories for a fair comparison.

Figure 7 shows the frequency responses for Case 1 in islanding and overloading events. It is shown in Figure 7a that the proposed UFLS recovered without overshooting compared to the references for Case 1. Table 5 summarizes a comparison of the proposed UFLS with those of previous studies for islanding events. It is shown that the proposed UFLS required the lowest number of shed loads and load sizing with four buses and 0.329 MW as compared to the UFLS<sub>PSI</sub> with six buses and 0.399 MW and Adaptive UFLS with eight buses and 0.517 MW. The proposed UFLS also had no frequency overshooting and was the fastest to reach 50.0 Hz of stable frequency at 16.47 s as compared to the UFLS<sub>PSI</sub>, which had an overshoot of 50.03 and reached the stable frequency at 25.23 s, and Adaptive UFLS, which had an overshoot of 50.18 Hz and reached the stable frequency at 30.50 s. Hence, the proposed UFLS was proven to achieve the best performance with respect to the islanding event for the base load.

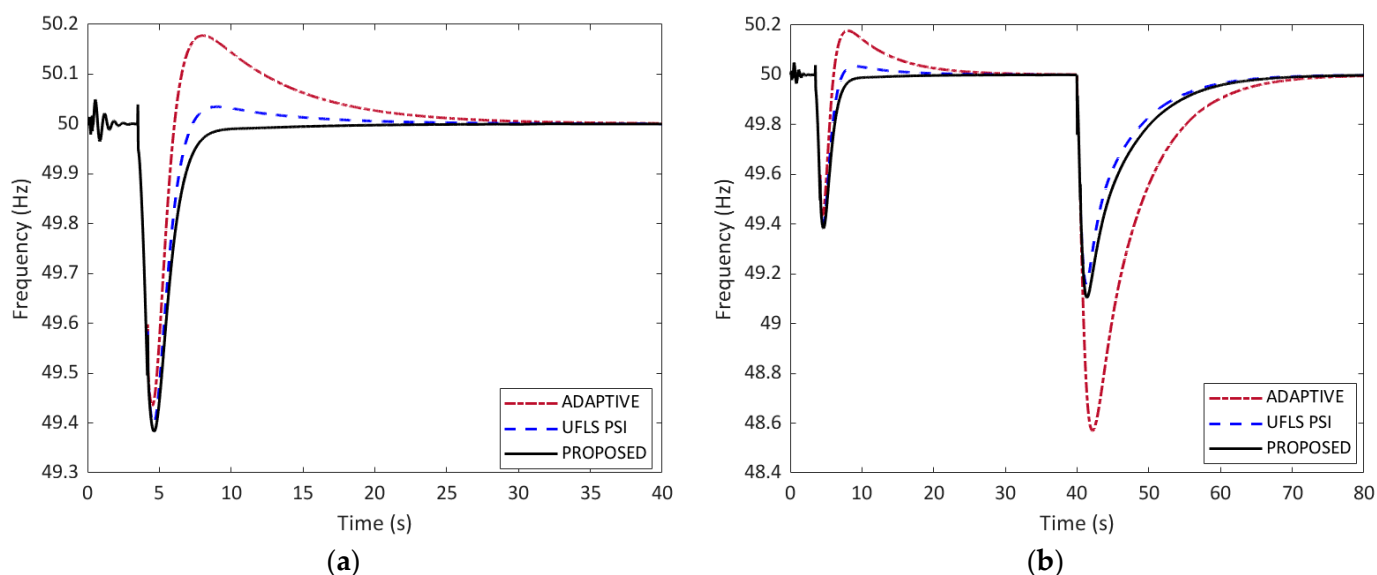


**Figure 7.** Frequency responses for Case 1 in (a) islanding events and (b) overloading events.

**Table 5.** Summary of frequency responses in islanding events for Case 1.

Results	Adaptive UFLS	UFLS Using PSI	Proposed UFLS
Loads shed (buses)	Nonvital: 1502, 1503, 1511, 1510, 1515, 1518, 1522, 1525 (8 buses)	Nonvital: 1502, 1511, 1510, 1518, 1519, 1525 (6 buses)	Nonvital: 1510, 1522, 1525, 1526 (4 buses)
Load shed size	0.517 MW	0.399 MW	0.329 MW
Frequency undershoot	49.43 Hz	49.39 Hz	49.38 Hz
Frequency overshoot	50.18 Hz	50.03 Hz	50.00 Hz
Time to reach 50.0 Hz	30.50 s	25.23 s	16.47 s

The performance of the proposed UFLS was further validated by considering the sudden increase in load demand in the overloading event at 40 s. As can be seen in Figure 7b, there was no significant frequency overshoot after the load was shed for all three

approaches: Adaptive UFLS, UFLS<sub>PSI</sub>, and the proposed UFLS. With regard to the frequency undershooting, the proposed UFLS recovered the quickest at 49.13 Hz as compared to UFLS<sub>PSI</sub> and Adaptive UFLS at 49.16 Hz and 48.57 Hz, respectively. Table 6 presents a summary of the frequency responses and load shedding for an overloading event. It is shown that the proposed UFLS required the lowest number of shed loads and load sizing with seven buses and 0.437 MW as compared to the UFLS<sub>PSI</sub> with eight buses and 0.453 MW and Adaptive UFLS with nine buses and 0.467 MW. However, the proposed UFLS took up to 68.03 s to recover the frequency to 50.0 Hz, which is slightly longer than UFLS<sub>PSI</sub> (67.58 s) but faster than Adaptive UFLS (73.57 s). Nevertheless, the difference in recovery time is not significant as compared to the number and size of loads shed as well as the frequency undershooting. Hence, the proposed UFLS was proven to achieve the best performance in the overloading event for the base loads.

**Table 6.** Summary of frequency responses in overloading events for Case 1.

Results	Adaptive UFLS	UFLS Using PSI	Proposed UFLS
Loads shed (buses)	Nonvital:1502, 1503, 1511, 1510, 1515, 1518, 1519, 1522, 1525 (9 buses)	Nonvital:1502, 1506, 1511, 1510, 1518, 1519, 1525, 1526 (8 buses)	Nonvital: 1506, 1511, 1510, 1519, 1522, 1525, 1526 (7 buses)
Load shed size	0.467 MW	0.453 MW	0.437 MW
Frequency undershoot	48.57 Hz	49.16 Hz	49.13 Hz
Frequency overshoot	50.00 Hz	50.00 Hz	50.00 Hz
Time to reach 50.0 Hz	73.57 s	67.58 s	68.03 s

#### 5.4. Comparison of the Frequency Responses and Load Shedding for Case 2

Figure 8 shows the frequency responses for Case 2 in the islanding and overloading events. In the islanding event, the proposed UFLS had a slight overshoot of 5.02 Hz; however, the frequency overshoot was substantially lower than those of the UFLS<sub>PSI</sub> and Adaptive UFLS, which were 50.40 Hz and 50.29 Hz, respectively, as shown in Figure 8a. A comparison of the frequency responses and load shedding in the previous studies is presented in Table 7. With a higher load demand in Case 2, the total load shed includes both nonvital and semi-vital loads for all approaches, as with more loads to be shed the power generation of the mini hydros is limited. The proposed UFLS required 13 buses of load sheds as compared to UFLS<sub>PSI</sub> with 12 buses and Adaptive UFLS with 14 buses. However, the proposed UFLS had the lowest load sizing with 0.969 MW compared to UFLS<sub>PSI</sub> and Adaptive UFLS with 1.126 MW and 1.079 MW, respectively. The proposed UFLS also had the fastest time to reach a stable frequency of 50.0 Hz at 16.48 s as compared to UFLS<sub>PSI</sub> and Adaptive UFLS at 29.93 s and 29.41 s, respectively. Hence, the proposed UFLS was proven to achieve the best performance in the islanding event for the peak load.

**Table 7.** Summary of frequency responses in islanding events for Case 2.

Results	Adaptive UFLS	UFLS Using PSI	Proposed UFLS
Loads shed (buses)	Nonvital: (11 buses) Semi-vital: 1509, 1514, 1524 (3 buses)	Nonvital: (11 buses) Semi-vital: 1505 (1 bus)	Nonvital: (11 buses) Semi-vital: 1509, 1514 (2 buses)
Load shed size	1.079 MW	1.126 MW	0.969 MW
Frequency undershoot	49.39 Hz	49.42 Hz	49.29 Hz
Frequency overshoot	50.29 Hz	50.40 Hz	50.02 Hz
Time to reach 50.0 Hz	29.41 s	29.93 s	16.48 s

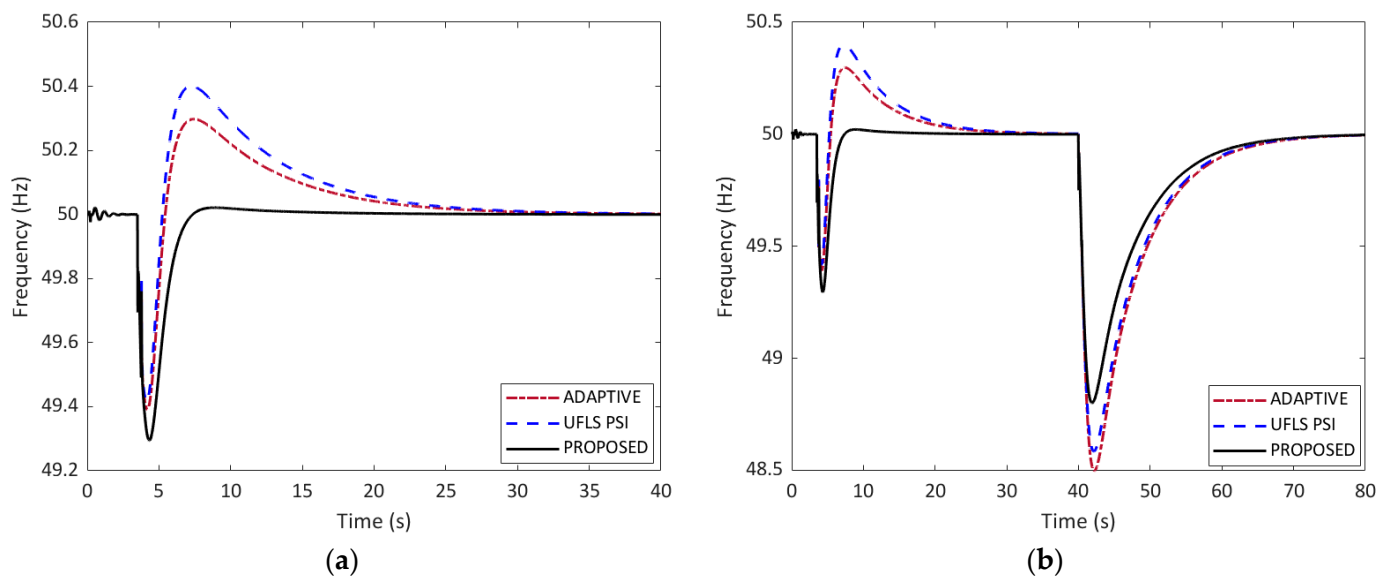


**Figure 8.** Frequency responses for Case 2 in (a) islanding events and (b) overloading events.

Figure 8b shows that the frequency responses of all three approaches for Case 2 in the overloading events at 40 s had no frequency overshoot after load shedding. With regard to frequency undershooting, the proposed UFLS recovered the quickest at 48.80 Hz as compared to UFLS<sub>PSI</sub> and Adaptive UFLS at 48.58 Hz and 48.49 Hz, respectively. Table 8 also shows that the proposed UFLS had the quickest time–frequency recovery, reaching 50.0 Hz in 73.04 s, as compared to UFLS<sub>PSI</sub> and Adaptive UFLS, which took 74.08 s and 74.88 s, respectively. However, the proposed UFLS required 15 buses of load sheds and 0.532 MW of load sizing, which was similar to Adaptive UFLS with 15 buses and 0.588 MW but higher than UFLS<sub>PSI</sub> with 13 buses and 0.471 MW. Nevertheless, the load-shedding performance of the proposed UFLS in the overloading event for the peak load was found to be better than that of the Adaptive UFLS, though comparable to that of UFLS<sub>PSI</sub>.

**Table 8.** Summary of frequency responses in overloading events for Case 2.

Results	Adaptive UFLS	UFLS Using PSI	Proposed UFLS
Loads shed (buses)	Nonvital: (11 buses) Semi-vital: 1509, 1513, 1514, 1524 (4 buses)	Nonvital: (11 buses) Semi-vital: 1505, 1507 (2 buses)	Nonvital: (11 buses) Semi-vital: 1509, 1514, 1520, 1524 (4 buses)
Load shed size	0.588 MW	0.471 MW	0.532 MW
Frequency undershoot	48.49 Hz	48.58 Hz	48.80 Hz
Frequency overshoot	50.00 Hz	50.00 Hz	50.00 Hz
Time to reach 50.0 Hz	74.88 s	74.08 s	73.04 s

5.5. Comparison of the Frequency Responses and Load Shedding for Case 3

Figure 9 shows a comparison of frequency responses for Case 1 in islanding and overloading events. In islanding events, the frequency response of the proposed UFLS had an overshoot of 50.28 Hz; however, the frequency overshoot was substantially lower than those of the UFLS<sub>PSI</sub> and Adaptive UFLS, which were 50.89 Hz and 50.79 Hz, respectively, as shown in Figure 9a. The higher-frequency overshoot in Case 3 compared to those in Cases 1 and 2 was due to the connection of PV generation. A comparison of the frequency responses and load shedding in the previous studies is presented in Table 9. In Case 3, the total load shed included both nonvital and semi-vital loads for all approaches, similar to Case 2, owing to the higher load demand. However, it was observed that the number and

size of the loads shed in Case 3 were smaller than those in Case 2 because PV generation was added to the system with mini hydro generation. Table 9 shows that the proposed UFLS shed fewer loads than Adaptive UFLS with 14 buses of load sheds; however, it was similar to UFLS<sub>PSI</sub> with 12 buses of load sheds. In contrast, the proposed UFLS shed the least amount of load sizing compared to UFLS<sub>PSI</sub> and Adaptive UFLS. The proposed UFLS also had the fastest time to recover to a stable frequency of 50.0 Hz, taking 30.11 s, as compared to UFLS<sub>PSI</sub> and Adaptive UFLS, which took 30.17 s and 30.15 s, respectively. In general, the proposed UFLS was proven to achieve the best performance compared with UFLS<sub>PSI</sub> and Adaptive UFLS. It was also shown that the proposed UFLS can select the appropriate load shed considering the variation in both load demand and power generation.

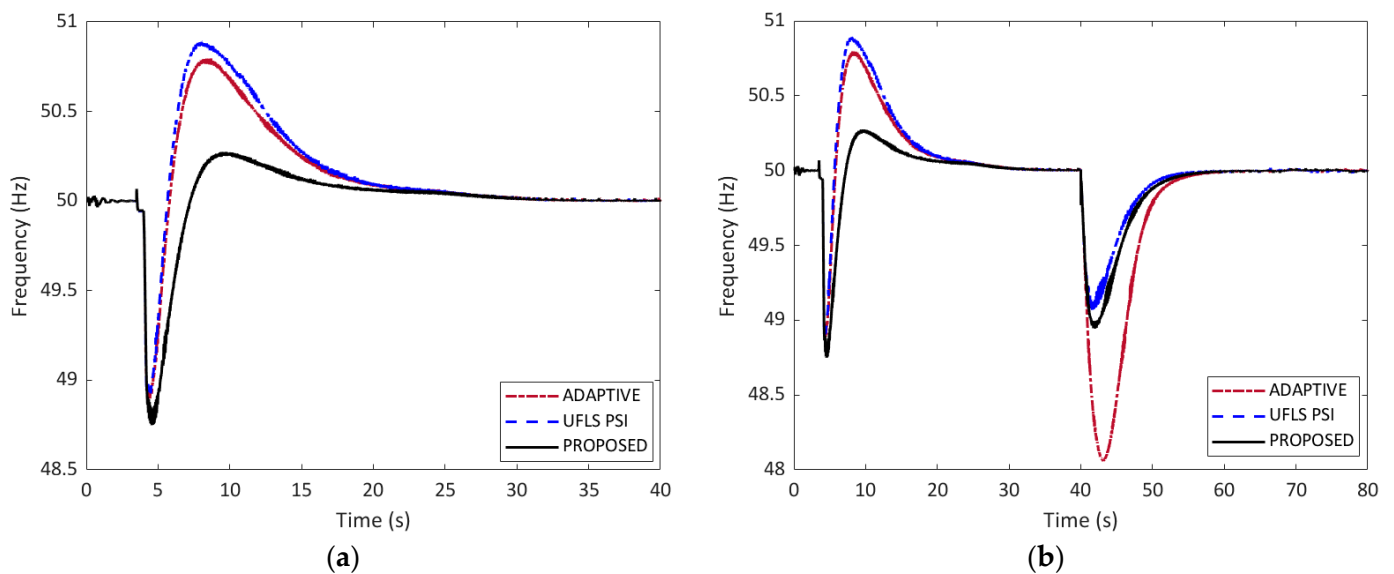


**Figure 9.** Frequency responses for Case 3 in (a) islanding events and (b) overloading events.

**Table 9.** Summary of frequency responses in islanding events for Case 3.

Results	Adaptive UFLS	UFLS Using PSI	Proposed UFLS
Loads shed (buses)	Nonvital: (11 buses) Semi-vital: 1509, 1514, 1524 (3 buses)	Nonvital: (11 buses) Semi-vital: 1505 (1 bus)	Nonvital: (11 buses) Semi-vital: 1509 (1 bus)
Load shed size	0.971 MW	1.026 MW	0.817 MW
Frequency undershoot	48.89 Hz	48.91 Hz	48.75 Hz
Frequency overshoot	50.79 Hz	50.89 Hz	50.28 Hz
Time to reach 50.0 Hz	30.15 s	30.17 s	30.11 s

In overloading events, the frequency responses after the overloading event at 40 s for all three approaches had a slight frequency overshoot of 50.02 Hz after load shedding, as shown in Figure 9b. With regard to frequency undershooting, the proposed UFLS recovered the quickest, at 48.80 Hz, as compared to UFLS<sub>PSI</sub> and Adaptive UFLS, at 47.18 Hz and 48.05 Hz, respectively. In general, the frequency recovered faster in Case 3 than in Case 2 for all three approaches due to the addition of PV generation in the test system. Table 10 shows that the proposed UFLS was the quickest to recover to the stable frequency of 50.0 Hz, at 54.93 s, as compared to UFLS<sub>PSI</sub> and Adaptive UFLS, which recovered at 56.17 s and 56.58 s, respectively. Despite being the highest load sizing to be shed, the proposed UFLS required 14 buses of load sheds, similar to UFLS<sub>PSI</sub>, which required fewer buses than Adaptive UFLS with 15 buses. Hence, the load-shedding performance of the proposed UFLS in the



overloading event for peak load with PV as additional generation was found to be better than that of Adaptive UFLS but comparable to that of UFLS<sub>PSI</sub>.

**Table 10.** Summary of frequency responses in overloading events for Case 3.

Results	Adaptive UFLS	UFLS using PSI	Proposed UFLS
Loads shed (buses)	Nonvital: (11 buses) Semi-vital: 1509, 1513, 1514, 1524 (4 buses)	Nonvital: (11 buses) Semi-vital: 1505, 1507, 1508 (3 buses)	Nonvital: (11 buses) Semi-vital: 1509, 1513, 1527 (3 buses)
Load shed size	0.552 MW	0.612 MW	0.699 MW
Frequency undershoot	48.06 Hz	49.06 Hz	48.94 Hz
Frequency overshoot	50.02 Hz	50.02 Hz	50.02 Hz
Time to reach 50.0 Hz	56.58 s	56.17 s	54.93 s

The performance of the proposed UFLS is summarised in Table 11, with the best results compared to those of Adaptive UFLS and UFLS<sub>PSI</sub>. Five results were obtained for each of the three cases for both islanding and overloading. The proposed UFLS achieved the best performance in 11 of the 15 recorded results (73.3%) for the islanding event and 9 of 15 results recorded for the overloading event (60.0%). Thus, it was proven that the proposed UFLS is one of the best options for the load-shedding scheme.

**Table 11.** Summary of the performance of the proposed UFLS.

Results	Islanding			Overloading		
	Case 1	Case 2	Case 3	Case 1	Case 2	Case 3
Load shed (bus)	√	X	√	√	X	√
Load shed size	√	√	√	√	X	X
Frequency undershoot	X	X	X	X	√	X
Frequency overshoot	√	√	√	√	√	√
Time to reach 50.0 Hz	√	√	√	X	√	√

√ indicates the best result in comparison with the systems described in [8,23] and [10].

### 5.6. Voltage Profile and Stability Index of The Proposed UFLS

The performance of the system after load shedding was also analyzed based on the voltage magnitudes of all buses. Figure 10 shows a comparison of the voltage profiles during islanding and after load shedding for all three case studies. The results show that the voltage profile improved significantly after the load was shed. Table 12 summarizes the voltage profiles for both the islanding and overloading events. It was shown that the system voltage recovered appropriately in the range of  $\pm 5\%$  per unit voltage for an 11 kV distribution system [22]. Figure 11 shows a comparison of the stability indices during islanding and after load shedding for all three case studies. A summary of the stability indices for both the islanding and overloading events is presented in Table 13. The results also showed that the stability index improved significantly after the load was shed.

**Table 12.** Summary of voltage profiles based on the proposed UFLS.

	Islanding	Case 1	Case 2	Case 3
Minimum Voltage (pu)	0.87	0.95	0.96	0.95
Maximum Voltage (pu)	0.95	1.01	1.01	1.02
Average Voltage (pu)	0.89	0.96	0.97	0.97
	Overloading	Case 1	Case 2	Case 3
Minimum Voltage (pu)	0.92	0.95	0.95	0.95
Maximum Voltage (pu)	0.98	1.00	1.00	1.01
Average Voltage (pu)	0.94	0.96	0.96	0.96

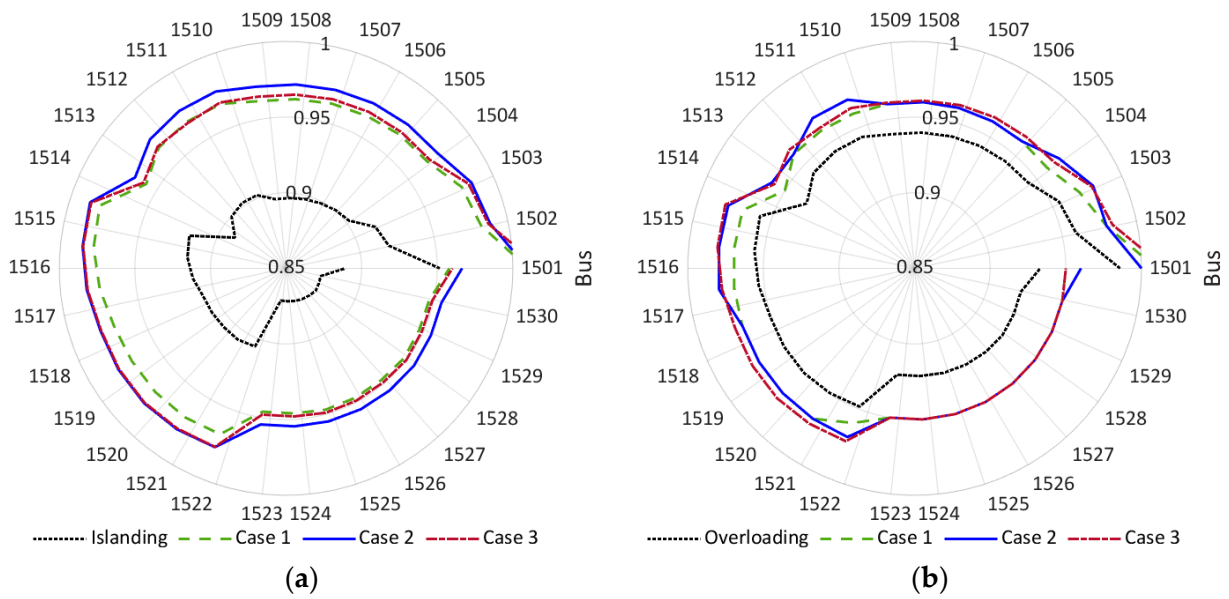


**Figure 10.** Voltage profile of the proposed UFLS in (a) islanding events and (b) overloading events.

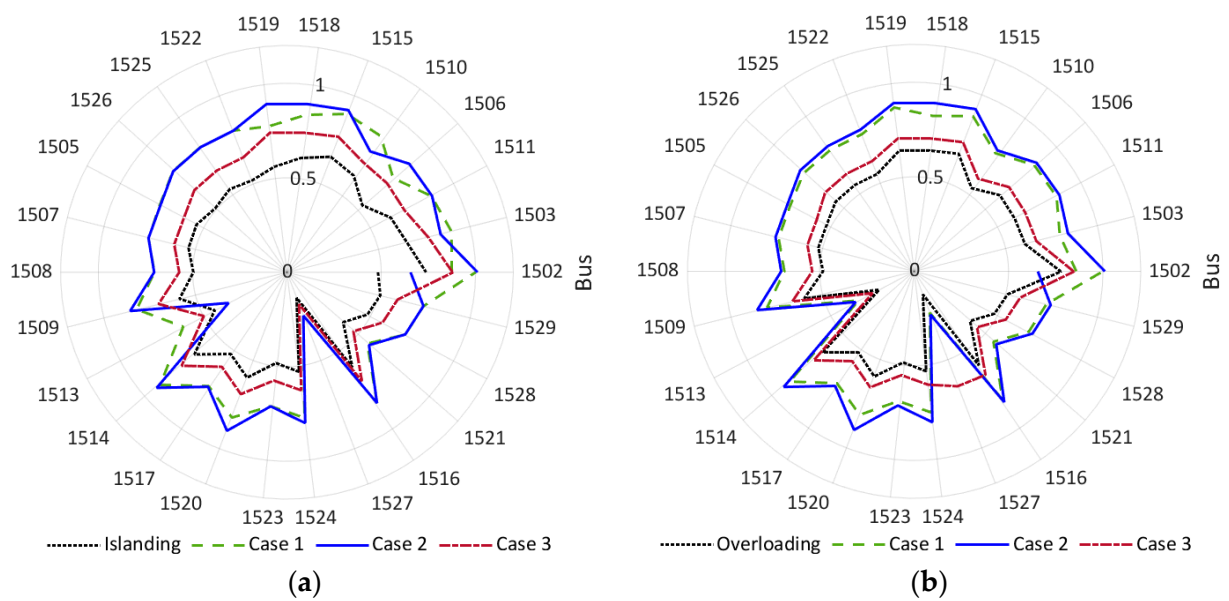


**Figure 11.** Stability indices of the proposed UFLS in (a) islanding events and (b) overloading events.

**Table 13.** Summary of stability indices based on the proposed UFLS.

	Islanding	Case 1	Case 2	Case 3
Minimum Voltage (pu)	0.14	0.24	0.25	0.18
Maximum Voltage (pu)	0.74	1.00	1.01	0.88
Average Voltage (pu)	0.54	0.77	0.77	0.65
	Overloading	Case 1	Case 2	Case 3
Minimum Voltage (pu)	0.13	0.23	0.24	0.25
Maximum Voltage (pu)	0.78	1.00	1.01	0.85
Average Voltage (pu)	0.55	0.75	0.77	0.63

## 6. Conclusions

In this study, a UFLS scheme for an islanded distribution network using a BAOA and WSM was proposed. The BAOA optimizes load shedding based on the minimum stability index and the power mismatch. The WSM ranks the loads to be shed based on various criteria. The effectiveness of the proposed UFLS was verified based on the frequency response and the amount of load shed. From the results, the proposed UFLS was proven to be effective in reducing frequency overshooting, improving frequency undershooting, and recovering more quickly than other approaches. The proposed UFLS was also proven to reduce the number and size of the loads shed. It was also observed that the proposed UFLS could appropriately recover system voltage. Hence, the performance of the proposed UFLS was proven to be effective in ensuring the reliability and stability of the power system. The proposed BAOA and WSM are viable solutions for addressing the UFLS scheme and can potentially be adapted to other power-system scenarios. Nevertheless, this study can be further enhanced by validating the UFLS scheme in real-time implementations. Without comprehensive automation control, any breakdown in the communication devices may lead to inaccurate load shedding in the proposed scheme.

**Author Contributions:** Conceptualization, H.M.R. and H.M.; methodology, H.M.R.; software, H.M. and N.N.M.; validation, H.M., N.N.M. and S.A.H.; formal analysis, H.M.R.; investigation, H.M.R.; resources, N.M.S.; data curation, N.M.S.; writing—original draft preparation, H.M.R.; writing—review and editing, S.A.H.; supervision, H.M., N.N.M. and M.F.S.; funding acquisition, H.M., L.W. and M.F.S. All authors have read and agreed to the published version of the manuscript.

**Funding:** This research was funded by Universiti Malaya under International Collaboration Grants ST027-2022 and IF022-2023.

**Data Availability Statement:** Data is unavailable due to privacy and ethical restrictions.

**Acknowledgments:** This research was supported by Asia Pacific University of Technology & Innovation (APU).

**Conflicts of Interest:** The authors declare no conflict of interest.

## Abbreviations

UFLS	Under-Frequency Load Shedding
AOA	Archimedes Optimization Algorithm
BAOA	Binary Archimedes Optimization Algorithm
WSM	Weighted Sum Method
DG	Distributed Generation
ROCOF	Rate of Change of Frequency
LSM	Load-Selection Module
LRM	Load-Ranking Module
LSCM	Load-Shed Controller Module

RCB Remote Circuit Breaker  
 SI Stability Index  
 SIC Stability Index Calculator  
 PSI Power Stability Index

## Appendix A

**Table A1.** Rankings of the loads to be shed based on WSM scores.

Nonvital (Bus)											
Rank	1	2	3	4	5	6	7	8	9	10	11
<b>Case 1 (Score)</b>	1525 (0.677)	1522 (0.676)	1526 (0.638)	1510 (0.549)	1511 (0.540)	1515 (0.283)	1518 (0.282)	1503 (0.268)	1502 (0.261)	1519 (0.224)	1506 (0.221)
<b>Case 2 (Score)</b>	1525 (0.546)	1522 (0.545)	1526 (0.521)	1510 (0.486)	1511 (0.480)	1515 (0.320)	1518 (0.319)	1503 (0.310)	1502 (0.306)	1519 (0.282)	1506 (0.280)
<b>Case 3 (Score)</b>	1510 (0.644)	1511 (0.631)	1525 (0.557)	1522 (0.556)	1526 (0.503)	1515 (0.277)	1518 (0.276)	1503 (0.256)	1502 (0.245)	1519 (0.196)	1506 (0.193)
Semi-Vital (Bus)											
Rank	12	13	14	15	16	17	19	20	21	22	
<b>Case 1 (Score)</b>	1509 0.089	1514 0.089	1524 0.089	1527 0.089	1513 0.089	1520 0.089	1517 0.089	1507 0.089	1523 0.089	1508 0.089	1505 0.089
<b>Case 2 (Score)</b>	1509 (0.130)	1514 (0.130)	1524 (0.130)	1513 (0.130)	1520 (0.130)	1517 (0.130)	1507 (0.130)	1523 (0.130)	1527 (0.130)	1508 (0.130)	1505 (0.130)
<b>Case 3 (Score)</b>	1509 (0.069)	1514 (0.069)	1524 (0.069)	1527 (0.069)	1513 (0.069)	1520 (0.069)	1517 (0.069)	1507 (0.069)	1523 (0.069)	1508 (0.069)	1505 (0.069)
Vital (Bus)											
Rank	23	24	25	26	27						
<b>Case 1 (Score)</b>	1516 (0.059)	1529 (0.059)	1528 (0.059)	1521 (0.059)	1501 (0.059)						
<b>Case 2 (Score)</b>	1516 (0.087)	1529 (0.087)	1528 (0.087)	1521 (0.087)	1501 (0.087)						
<b>Case 3 (Score)</b>	1516 (0.046)	1529 (0.046)	1528 (0.046)	1521 (0.046)	1501 (0.046)						

## References

1. Tenaga, S. *A Malaysia Energy Statistics Handbook 2020*; Energy Commission: Putrajaya, Malaysia, 2020.
2. Authority Malaysia, S.E.D. *Malaysia Renewable Energy Roadmap*; SEDA: Kuala Lumpur, Malaysia, 2021.
3. Noor, F.; Arumugam, R.; Vaziri, M.Y. Unintentional islanding and comparison of prevention techniques. In Proceedings of the 37th Annual North American Power Symposium, Ames, IA, USA, 25 October 2005; pp. 90–96.
4. Laghari, J.; Mokhlis, H.; Karimi, M.; Bakar, A.; Mohamad, H. Computational Intelligence based techniques for islanding detection of distributed generation in distribution network: A review. *Energy Convers. Manag.* **2014**, *88*, 139–152. [\[CrossRef\]](#)
5. Sigrist, L.; Rouco, L.; Echavarren, F.M. A review of the state of the art of UFLS schemes for isolated power systems. *Int. J. Electr. Power Energy Syst.* **2018**, *99*, 525–539. [\[CrossRef\]](#)
6. Karimi, M.; Mohamad, H.; Mokhlis, H.; Bakar, A. Under-frequency load shedding scheme for islanded distribution network connected with mini hydro. *Int. J. Electr. Power Energy Syst.* **2012**, *42*, 127–138. [\[CrossRef\]](#)
7. Seyedi, H.; Sanaye-Pasand, M. New centralised adaptive load-shedding algorithms to mitigate power system blackouts. *IET Gener. Transm. Distrib.* **2009**, *3*, 99–114. [\[CrossRef\]](#)
8. Terzija, V. Adaptive Underfrequency load shedding based on the magnitude of the disturbance estimation. *IEEE Trans. Power Syst.* **2006**, *21*, 1260–1266. [\[CrossRef\]](#)
9. Alhelou, H.H.; Golshan, M.E.H.; Njenda, T.C.; Hatziaergyriou, N.D. An overview of UFLS in conventional, modern, and future smart power systems: Challenges and opportunities. *Electr. Power Syst. Res.* **2020**, *179*. [\[CrossRef\]](#)
10. Sapari, N.M.; Mokhlis, H.; Abu Bakar, A.H.; Mohamad, H.; Laghari, J.A.; Dahalan, M.R.M. Load shedding scheme based on rate of change of frequency and ranked stability index for islanded distribution system connected to mini hydro. *IEEJ Trans. Electr. Electron. Eng.* **2017**, *12*, 347–356. [\[CrossRef\]](#)
11. Sun, M.; Liu, G.; Popov, M.; Terzija, V.; Azizi, S. Underfrequency load shedding using locally estimated RoCof of the center of inertia. *IEEE Trans. Power Syst.* **2021**, *36*, 4212–4222. [\[CrossRef\]](#)
12. Jallad, J.; Mekhilef, S.; Mokhlis, H.; Laghari, J.; Badran, O. Application of hybrid meta-heuristic techniques for optimal load shedding planning and operation in an islanded distribution network integrated with distributed generation. *Energies* **2018**, *11*, 1134. [\[CrossRef\]](#)

13. Sarwar, S.; Mokhlis, H.; Othman, M.; Shareef, H.; Wang, L.; Mansor, N.N.; Khairuddin, A.S.M.; Mohamad, H. Application of polynomial regression and MILP for under-frequency load shedding scheme in islanded distribution system. *Alex. Eng. J.* **2022**, *61*, 659–674. [[CrossRef](#)]
14. Yusof, N.A.; Rosli, H.M.; Mokhlis, H.; Karimi, M.; Selvaraj, J.; Sapari, N.M. A new under-voltage load shedding scheme for islanded distribution system based on voltage stability indices. *IEEJ Trans. Electr. Electron. Eng.* **2017**, *12*, 665–675. [[CrossRef](#)]
15. Larik, R.M.; Mustafa, M.W.; Aman, M.N.; Jumani, T.A.; Sajid, S.; Panjwani, M.K. An improved algorithm for optimal load shedding in power systems. *Energies* **2018**, *11*, 1808. [[CrossRef](#)]
16. Małkowski, R.; Nieznański, J. Underfrequency load shedding: An innovative algorithm based on fuzzy logic. *Energies* **2020**, *13*, 1456. [[CrossRef](#)]
17. Talaat, M.; Hatata, A.; Alsayyari, A.S.; Alblawi, A. A smart load management system based on the grasshopper optimization algorithm using the under-frequency load shedding approach. *Energy* **2020**, *190*, 116423. [[CrossRef](#)]
18. Rosli, H.M.; Mokhlis, H.; Mansor, N.N.; Sapari, N.; Halim, S.A. A Modified DEP and AHP for Load Shedding Scheme of Islanded Distribution System Incorporating Stability Index. *J. Electr. Eng. Technol.* **2022**, *17*, 1581–1592. [[CrossRef](#)]
19. Hashim, F.A.; Hussain, K.; Houssein, E.H.; Mabrouk, M.S.; Al-Atabany, W. Archimedes optimization algorithm: A new metaheuristic algorithm for solving optimization problems. *Appl. Intell.* **2021**, *51*, 1531–1551. [[CrossRef](#)]
20. Kennedy, J.; Eberhart, R.C. A discrete binary version of the particle swarm algorithm. In Proceedings of the Computational Cybernetics and Simulation 1997 IEEE International Conference on Systems, Man, and Cybernetics, Orlando, FL, USA, 12–15 October 1997; Volume 5.
21. Eminoglu, U.; Hocaoglu, M.H. A voltage stability index for radial distribution networks. In Proceedings of the 42nd International Universities Power Engineering Conference, Brighton, UK, 4–6 September 2007; pp. 408–413.
22. Berhad, T.N. *Electricity Supply Application Handbook*, 2nd ed.; Tenaga Nasional Berhad: Kuala Lumpur, Malaysia, 2007.
23. Terzija, V.; Koglin, H.J. Adaptive underfrequency load shedding integrated with a frequency estimation numerical algorithm. *IEE Proc. Gener. Transm. Distrib.* **2002**, *149*, 713–718. [[CrossRef](#)]

**Disclaimer/Publisher’s Note:** The statements, opinions and data contained in all publications are solely those of the individual author(s) and contributor(s) and not of MDPI and/or the editor(s). MDPI and/or the editor(s) disclaim responsibility for any injury to people or property resulting from any ideas, methods, instructions or products referred to in the content.